Anti-CD19 CAR T Cells That Secrete a Biparatopic Anti-CLEC12A Bridging Protein Have Potent Activity Against Highly Aggressive Acute Myeloid Leukemia *In Vitro* and *In Vivo*

Paul D. Rennert, Fay J. Dufort, Lihe Su, Tom Sanford, Alyssa Birt, Lan Wu, Roy R. Lobb, and Christine Ambrose

ABSTRACT

Refractory acute myeloid leukemia (AML) remains an incurable malignancy despite the clinical use of novel targeted therapies, new antibody-based therapies, and cellular therapeutics. Here, we describe the preclinical development of a novel cell therapy that targets the antigen CLEC12A with a biparatopic bridging protein. Bridging proteins are designed as "CAR-T cell engagers," with a CAR-targeted protein fused to antigen binding domains derived from antibodies. Here, we created a CD19-anti-CLEC12A bridging protein that binds to CAR19 T cells and to the antigen CLEC12A. Biparatopic targeting increases the potency of bridging protein-mediated cytotoxicity by CAR19 T cells. Using CAR19 T cells that secrete the bridging protein we demonstrate potent activity against aggressive leukemic cell lines *in vivo*. This CAR-engager platform is facile and modular, as illustrated by activity of a dual-antigen bridging protein targeting CLEC12A and CD33, designed to counter tumor heterogeneity and antigen escape, and created without the need for extensive CAR T-cell genetic engineering. CAR19 T cells provide an optimal cell therapy platform with well-understood inherent persistence and fitness characteristics.

Introduction

Patient-derived T cells expressing an anti-CD19 chimeric antigen receptor (CAR19) are approved for the treatment of advanced, refractory hematologic malignancies and can provide long-term remissions and apparent cures for some patients with no other therapeutic options, a stunning achievement (1). This success has spurred intensive work on CAR T-cell therapies for diverse indications. For example, approval of CAR T cells that target the B-cell maturation antigen (BCMA) for the treatment of relapsed or refractory (r/r) multiple myeloma is expected (2).

Challenges limit the use of cell therapies. Relapses are a critical issue. Approximately half of all patients who respond to CAR19 T-cell therapy relapse 6 months or less after treatment and the majority of patients who receive a BCMA-targeting CAR eventually relapse (3, 4). CAR T-cell manufacturing remains a logistically complex and expensive process (5). Toxicity from cytokine release syndrome and immune effector cell–associated neurotoxicity syndrome complicate patient care and increase associated health care costs (6). Finally, many tumor antigens are also expressed on critical normal cells and tissues, putting patients at risk of off-

tumor, on-target toxicity (7, 8). These issues suggest that simple and robust solutions are needed as cell therapeutics are deployed across diverse indications.

We have shown that CD19-containing bridging proteins (BP) can redirect CAR19 T cells to target diverse antigens *in vitro* (9). Furthermore, CAR19 T cells engineered to secrete BPs retained their ability to expand and proliferate in response to CD19 antigen (10). Finally, CAR19 T cells that secreted an CD19-BP targeting Her2 eradicated Her2-positive tumors *in vivo* (10).

Here we use the CAR19 T cells and the BP technology to target acute myeloid leukemia (AML). Despite the arrival of diverse new classes of therapeutics for treatment in combination with chemotherapy outcomes remain poor for patients who are refractory to initial induction and consolidation therapy or who relapse (11). Only a small number of patients achieve a stringently defined complete remission that is essential for successful hematopoietic stem cell transplantation and a possible cure (12). Therefore, the unmet need in AML remains very high.

The expression pattern of AML antigens complicates the development of advanced therapies (13). Ideally, target antigens will be expressed on both AML blast cells and AML leukemic stem cells (LSC) that can cause relapse, with limited expression on normal cells (14, 15). Here we target the antigens CLEC12A and CD33. CLEC12A is expressed on AML blasts and LSC but normal cell expression is limited, and early-stage hematopoietic stem and progenitor cells are negative (16). Similarly, high CD33 expression on AML blasts and LSC is well established, while normal expression is lower, and limited to myeloid lineage cells, including common myeloid progenitor cells, but not multi-progenitor stem cells (17).

We describe a novel targeting system using CAR19 T cells and a unique secreted BP, allowing the CAR19 T cell to bind AML antigens. We present *in vitro* and *in vivo* preclinical analyses of a biparatopic CLEC12A-targeting BP and of CAR19 T cells that secrete the BP. Finally, we characterize a multi-antigen BP that simultaneously targets

CD33 and CLEC12A. Notably, this technology leverages the extensive knowledge accumulated regarding the activity and production of CAR19 T cells, simplifying development.

Materials and Methods

Here we briefly summarize novel protocols. Detailed protocols are available at https://www.protocols.io/file/c9bhbje6x.docx and in the Supplementary Materials and Methods section.

Human cell lines

All cell lines were obtained directly from suppliers and used in low passage number from stored cell banks. ATCC and DSMZ (Braunschweig, Germany) provided certificates of analysis including cell line verification. DSMZ and ATCC maintain comprehensive databases of short tandem repeats cell line profiles used to verify their commercial cell lines. U937, 293T, Molm14, Nalm6 (ATCC) and PL-21, OCI-AML2 and OCI-AML5 (DSMZ) were cultured per supplier instructions. All cell lines were tested for *Mycoplasma* and, prior to *in vivo* use, for murine virus contamination, and were negative (SBH Sciences). Luciferase expressing lines were generated via lentivirus (GeneCopoeia) and puromycin selection.

BP constructs

BP constructs were cloned into pcDNA3.1+ hygro (Invitrogen). Single-chain fragment variable (scFv) domains were cloned from antibody sequences. CD19-scFv contained the CD19 ECD and an anti-CLEC12A scFv CD19-1B12 contained an N terminal stabilized CD19 ECD (9) and the llama 1B12-VH sequence. 2H3-CD19 contained the llama 2H3-VH sequence, a C terminal–stabilized CD19 ECD (9). scFv-2H3-CD19 contained the anti-CLEC12A scFv, the 2H3 variable heavy chain (VH) and a C terminal–stabilized CD19. Anti-CD33-CD19 contained a chemically synthesized anti-CD33 scFv and a C terminal–stabilized CD19 ECD. Anti-CD33-CLEC12A-CD19 contained the anti-CD33 scFv, the 2H3 VH, and the C terminal–stabilized CD19 ECD. Constructs were His-tagged. G4S linkers were used between domains.

CAR constructs

The anti-CD19 CAR sequence CAR19 has been described previously (9). The anti-CLEC12A CAR construct CAR-CLEC12A-2H3 contained the 2H3 sequence with the same stalk and intracellular domain as used in the CAR19. The anti-CLEC12A CAR construct CAR-CLEC12A-scFv used the anti-CLEC12A scFv. The following constructs were chemically synthesized by Lentigen Technologies (Gaithersburg) and cloned into a lentiviral vector containing an MSCV promoter. All contained the CAR19 sequence, a P2A site, and then a BP sequence. CAR19-scFv-BP contained the CD19-scFv BP. CAR19-2H3-BP contained the 2H3-CD19 BP. CAR19-bi-BP contained the ScFv-2H3-CD19 BP. Viral particles were produced by Lentigen Technologies.

CAR T production

CD3-positive human primary T cells were cultivated in ImmunoCult-XF T-cell expansion medium (serum/xeno-free) supplemented with 20 IU/mL IL2 at a density of 3×10^5 cells/mL, activated with anti-CD3/anti-CD28 T-cell Activator reagent (STEMCELL Technologies) and transduced on day 1 with lentiviral particles in the presence of $1\times$ Transdux (SBI). Cells were harvested on day 10. The percent CAR expression was measured by anti-Flag or CD19-Fc detection. Briefly, 500,000 cells were incubated with

anti-FLAG antibody followed by anti-rabbit APC (both at 1:100 dilution, Thermo Fisher Scientific) or 0.25 µg/mL CD19-Fc (R&D Systems) followed by 1:200 dilution of anti-Fc gamma (Jackson ImmunoResearch). Cells were fixed with 2% paraformaldehyde and the percent positive cell populations was measured using a BD Accuri C6 flow cytometer.

Assays for BP binding to CLEC12A protein and cells

ELISA assays were performed to determine the binding of the various BPs to CLEC12A. Plates were coated with 1.0 µg/mL anti-CD19 FMC63 antibody (Novus Biological) in 0.1 mol/L carbonate, pH 9.5 overnight at 4°C. The plate was blocked with 0.3% non-fat milk in TBS (0.1 mol/L Tris, 0.5 mol/L NaCl) for 1 hour at room temperature. After washing three times in TBST (TBS/0.05% Tween20), fusion proteins were titrated using 3-fold dilutions in TBS/1% BSA and incubated 1 hour at room temperature. Biotinylated CLEC12A and streptavidin-HRP (horseradish peroxidase) were used to detect binding. CLEC12A (Sino Biological) was biotinylated using a EZ-Link Micro Sulfo-NHS-LC kit (Thermo Fisher Scientific) and added at 0.1 µg/mL and incubated for 1 hour at room temperature, followed by streptavidin-HRP (Thermo Fisher Scientific) at 1:2,000 dilution. The HRP-coupled reagents were incubated at room temperature for 1 hour. Plates were washed between all incubation steps with TBST. 1-Step Ultra TMB-ELISA solution (Thermo Fisher Scientific) was added and the plate read at 405 nm. Data were analyzed using Softmax software where curves were fit using a four-parameter logistic regression to calculate the EC_{50}.

BP binding to cells was assayed using flow cytometry with anti-His-PE or anti-CD19 FMC63-PE (9). 293T cells were transfected with GenScript cDNAs for CLEC12A (K variant OHu09814D), CLEC1A (OHu27138D), or CLEC12B (OHu13983B), using Lipofectamine 2000 as directed (Thermo Fisher Scientific). The CLEC12A Q variant was generated by PCR. Stable cell lines were selected using antibiotic resistance.

Epitope mapping

The 2H3-VH and the anti-CLEC12A scFv were purified. CLEC12A was purchased (Sino Biological). The epitopes of the scFv and 2H3-VH were determined using mass spectrometry by CovalX.

In vivo studies

All animal studies were performed in an Association for Assessment and Accreditation of Laboratory Animal Care International (AALAC)-accredited vivarium under an approved Institutional Animal Care and Use Committee protocol at the Tuft's University Cummings School of Veterinary Medicine (North Grafton, MA). All studies used 6–8 weeks old NSG (NOD.Cg-*Prkdc^{scid} Il2rg^{tm1Wjl}*/SzJ) mice (Jackson Laboratories) which were rested for 4 days prior to study initiation.

For the CD19-positive cell model, 1×10^6 Nalm6-luciferase cells were injected intravenously in NSG mice. Three days later, the mice were injected intravenously with 2, 5, or 10×10^6 CAR T cells, untransduced (UTD) cells, or no cells. The group size was $N = 5$ except the NA group was 3 animals. The mice were followed for 21 days by imaging as detailed below.

For the first U937-luc study, NSG mice were injected intravenously with 1×10^5 cells. On day 3, 1×10^7 T cells (CLEC12A-bridging CAR19, CAR-CLEC12A, or UTD) were delivered intravenously ($N = 10$ mice/cohort). For analysis, animals received luciferin 150 mg/kg intraperitoneally, were anesthetized with isoflourane and imaged (PerkinElmer IVIS 200).

For the dose response, mice received 2.5×10^4 U937-luc cells intravenously and 2×10^6, 5×10^6 or 1×10^7 cells CAR T cells were injected on day 3 ($N = 5$ mice/cohort).

To compare CAR activity in the U937 model, 1×10^7 CAR T cells were injected intravenously into the mice 3 days after tumor cell injection (2.5×10^4; $N = 5$ mice/cohort). The study was terminated on day 27 as control mice had to be euthanized.

For the PL21-luc study, 10^6 cells were injected intravenously and 8 days later, 1×10^7 CAR T cells were injected intravenously. The cohort size was $N = 6$.

Results

BPs created using the CD19 ECD and scFv and VHs from anti-CLEC12A antibodies

We previously described wildtype and stabilized mutant forms of the CD19 ECD fused to binding domains to create BPs that redirect CAR19 T cells to kill Her2-, BCMA- or CD20-expressing cell lines *in vitro* (9) and Her2-positive tumors *in vivo* (10).

Here we create BPs to target AML. First, we cloned the CD19 ECD in frame with an anti-CLEC12A scFv (**Table 1**; ref. 18). The CD19-scFv BP bound to stably transfected 293T-CLEC12A cells with an EC_{50} of 1 nmol/L (Supplementary Fig. S1A) and to U937 AML cells with an EC_{50} of approximately 10 nmol/L (9). Similar affinity was measured in an anti-CD19-capture/CLEC12A-detection ELISA format (EC_{50} ∼2.5 nmol/L; Supplementary Fig. S1B). Thus, the scFv-based BP bound to both anti-CD19 antibody and to CLEC12A antigen with low nmol/L affinity.

Immunized llamas generated single domain antibodies, sdAbs, encoding VHs (19). Two VH clones, 2H3 and 1B12, bound CLEC12A with high affinity in ELISA and flow cytometry assays (Supplementary Table S1). These VH clones were used to create BPs using stabilized CD19 ECDs (C6.2 and NT.1; ref. 9).

The two VH-based BPs bound to CLEC12A with sub-nmol/L affinities, at least 10-fold lower than the scFv-based BP in the same assay (**Fig. 1A**; **Table 2**). The VH-based BPs bound U937 cells in flow cytometry assays with low pmol/L affinity (**Fig. 1B**; **Table 2**).

Epitope mapping of anti-CLEC12A antibodies

In a CLEC12A competition ELISA, 2H3 and 1B12 revealed overlapping epitopes, but did not block the scFv (Supplementary Table S2; a reading of ≥0.3 = specific binding). We then performed mass spectrometric epitope mapping analyses of the scFv and the 2H3 VH-binding domains complexed with purified CLEC12A. Both the scFv and the 2H3 VH bound to the C-terminal region of CLEC12A and had one contact residue in common (**Fig. 1C**). Thus, the epitopes were adjacent but distinct.

Table 1. BPs and CAR constructs.

BP composition	Nomenclature
Wildtype CD19-ECD–anti-CLEC12A scFv	CD19-scFv
Stabilized CD19-ECD–anti-CLEC12A 2H3-VH	CD19-2H3
Anti-CLEC12A 1B12-VH–stabilized CD19-ECD	1B12-CD19
Anti-CLEC12A scFv–anti-CLEC12A 2H3-VH–stabilized CD19	scFv-2H3-CD19
Anti-CD33 scFv–stabilized CD19	CD33-CD19
Anti-CLEC12A 2H3-VH–anti-CD33 scFv–stabilized CD19	2H3-CD33-CD19

Note: The table presents a description of BPs created.

Genomic analyses indicated that the 2H3 epitope contained allelic variants. The CLEC12A gene can encode either a lysine (K) or glutamine (Q) at amino acid 244 (UniProtKB accession no. Q5QGZ9). The global allele frequencies are 0.35 (K variant) and 0.65 (Q variant). In Asia the frequency of the Q variant reaches 0.85 (NCBI, Gene ID: 160364). We tested binding of the CD19-scFv and CD19-2H3 BPs to 293T transfectants expressing the K or Q variant. Both were highly expressed on the transfected cell surface (Supplementary Fig. S2A).

The CD19-2H3 BP bound the 244Q variant with very high affinity (4.8 pmol/L; **Fig. 1D**) but did not bind to the 244K variant. The CD19-scFv BP bound similarly to both 244K and 244Q variants (0.7 and 2 nmol/L, respectively; **Fig. 1D**). The mass spectrometric epitope mapping analysis showed that amino acid 244 is not a direct contact site but lies within the 2H3 epitope (**Fig. 1C**). The 244K residue likely perturbs the structural presentation of the 2H3 epitope. The allele frequencies indicate that >85% of individuals will express at least one copy of the 244Q variant.

A biparatopic BP binds to CLEC12A-expressing cells with high affinity

The region of a protein recognized by an antibody is called the epitope; the region within an antibody hypervariable domain that binds to the epitope is called the paratope. Monoparatopic binding is to one epitope; biparatopic binding is to two epitopes. We designed a biparatopic BP using the scFv and 2H3, linked to a stabilized CD19 ECD at the C-terminus, thus scFv-2H3-CD19 (**Table 1**).

Unexpectedly, the biparatopic BP bound to transfected 293T cells expressing the 244K variant with high affinity in a flow cytometry assay, with an $EC_{50} = 43$ pmol/L (**Fig. 1D**). This result suggests that linking the 2H3 VH and the scFv in the biparatopic BP enhanced binding to the 244K allele. We speculate that stabilization occurred between the adjacent 2H3 and scFv epitopes. Understanding the precise nature of this phenomenon will require more extensive mutational and molecular modeling studies.

We tested the biparatopic BP binding to 293T cells transfected with CLEC1 and CLEC12B, which have the highest sequence homology to CLEC12A (**Fig. 1C**). No binding was detected (Supplementary Fig. S2B). These results showed that the biparatopic BP binds CLEC12A with high affinity and specificity.

The biparatopic BP induces potent cytotoxicity in the presence of CAR19 T cells

We evaluated BP binding to U937 cells which are CLEC12A bright by flow cytometry (see Supplementary Fig. S3). The biparatopic BP bound with an $EC_{50} = $ ∼8 pmol/L, which is much greater affinity than achieved with either of the monoparatopic BPs (**Fig. 1E**; **Table 2** includes summary statistics).

The BPs induced cytotoxicity in the presence of CAR19 T cells and U937-luc cells. Increasing doses of the different BPs and CAR19 T cells were added to U937-luc cells to give a effector to target (E:T) ratio of 10:1. The extent of tumor cell death was measured by a decrease in luciferase signal after 48 hours; the biparatopic BP induced cytotoxicity with a derived IC_{50} value = 1 pmol/L (**Fig. 1F**; **Table 2**). Therefore, both the binding affinity and the cytotoxic potency of the biparatopic BP were significantly better than the monoparatopic BPs derived using scFv or the VH clones (**Table 2**). The biparatopic BP also had potent binding and cytotoxic activity against additional AML cell lines that express CLEC12A including AML2, AML5, and PL21 (Supplementary Table S3; Supplementary Fig. S3B and S3C).
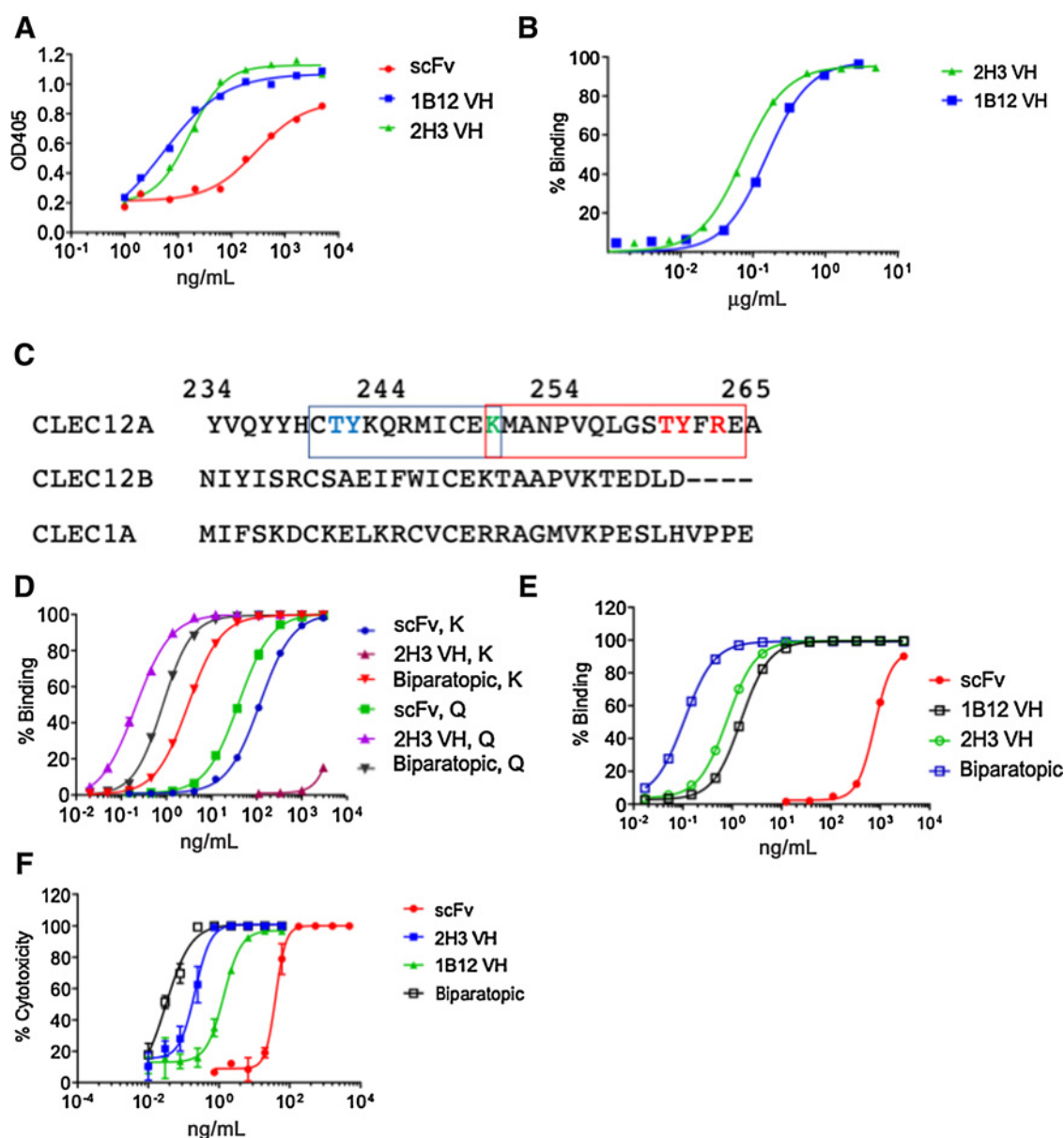
Figure 1.
BP binding affinities and cytotoxic activities. CD19-BPs are identified by the antibody domain (scFv, 2H3, 1B12); the biparatopic is scFv-2H3-CD19 ECD. **A,** Dose–response ELISA using anti-CD19–coated plates to capture BPs and biotinylated CLEC12A for detection. **B,** Dose–response flow cytometry assay using U937 cells to bind BPs and anti-CD19-PE for detection. **C,** CLEC12A epitopes defined for the scFv (red box) and 2H3 (blue box) binding to CLEC12A. The corresponding region of CLEC12B and CLEC1A are shown below the CLEC12A sequence. **D,** Analysis of binding of different BPs to amino acid 244 allelic variants of CLEC12A. **E,** Dose–response flow cytometry assay using U937 cells. **F,** Dose–response cytotoxicity assays using U937-luc cells and CAR19 T cells. Summary statistics are given in **Table 2**.

BPs function as CAR-T engagers, with activity similar in principle to CD3-based T-cell engagers (20). It was critical to demonstrate that the engager protein did not interfere with CAR T-cell function by blocking antigen binding, inducing functional exhaustion through tonic signaling or triggering cell death (21, 22). We used cytotoxicity assays in which the components—CAR19 T cells, BPs, and CLEC12A-positive U937 target tumor cells—were premixed in different combinations to evaluate these issues. CAR19 T cells were preincubated with excess BP (1 mg/mL) before being added to the target tumor cells, or, the U937

tumor cells were preincubated with excess BP before being added to the CAR19 T cells, or, as the positive control, all three components were added to the assay simultaneously. There was no difference in the extent of cytotoxicity induced under these conditions for any BP (**Fig. 2A**). The exact same conditions were used with Nalm6 cells and there was no difference in the extent of cytotoxicity induced, in this case via direct engagement of CD19 (**Fig. 2B**). Therefore, excess BP does not interfere with the ability of CAR19 T cells to bind to target antigen and trigger cytotoxicity.

Table 2. Characterization of BPs.

Bridging protein	U937 cell binding (EC$_{50}$)		U937 cell cytotoxicity (IC$_{50}$)	
	ng/mL	pmol/L	ng/mL	pmol/L
CD19-scFv[a]	570 (4)	10,200 (100)	54.9 (13)	980 (226)
1B12-CD19[b]	8 (0.4)	164 (32)	1.3 (0.3)	28.2 (3)
CD19-2H3[b]	4 (0.8)	90 (20)	0.34 (0.1)	7.3 (1.8)
scFv-2H3-CD19[a] (biparatopic)	0.6 (0.1)	8 (2)	0.04 (0.02)	0.6 (0.2)

Note: Binding affinities and cytotoxic activities of CD19-containing BPs created using different anti-CLEC12A binding domains. Flow cytometry was used to measure dose-responsive binding to U937 cells and calculate EC$_{50}$ values. Cytotoxicity activity against target U937-luc cells was calculated from the reduction of luciferase signal after incubation with CAR19 T cells and a titration of each BP. The IC$_{50}$ data were calculated from the cytotoxicity results. Data are shown as mean (SD) and are derived from $n > 3$ independent experiments.
[a] $= P < 0.01$ for all comparisons of scFv versus 2H3 or 1B12 BPs and for all comparisons of the biparatopic BP versus other BPs.
[b] $= P < 0.05$ for comparisons of the 1B12 versus 2H3 BPs.

CAR T cells can express an anti-CD19 CAR domain and secrete functional BPs

We next created "CLEC12A-bridging CAR19 T cells" by adding a P2A cleavage site and a BP sequence downstream of a CAR19 sequence. Lentiviral particle transduced donor T cells were used to create CAR19 T cells secreting the monoparatopic BPs (CAR19-scFv-BP T cells and CAR19-2H3-BP T cells) and the biparatopic BP (CAR19-bi-BP T cells). The latter construct was made with and without an N-terminal Flag tag on CAR domain and a C-terminal His tag on the BP (**Table 1**). We made CAR T cells that target CLEC12A, using the scFv or the 2H3 sequences, thus, CAR-CLEC12A-scFv and CAR-CLEC12A-2H3, respectively (all CAR and CAR-BP sequences are in Supplementary Data S1). CAR expression by CLEC12A-bridging CAR19 and CAR-CLEC12A T cells, derived from different donors, was assayed by flow cytometry after transduction and 10 days of cell expansion. CAR expression was variable but was routinely >45% (Supplementary Table S4).

We first assessed the cytotoxic activity of CLEC12A-bridging CAR19 T cells against CD19-positive B cell lines. CAR19-2H3-BP and CAR19-bi-BP T cells had similar cytotoxic activity as CAR19 T cells against Nalm6 cells and JeKo-1 cells (**Fig. 2C** and **D**). These data show that the anti-CD19 CAR domain is not blocked by secreted BPs and can bind to CD19, to induce cytotoxicity.

Redirected cytotoxicity was evaluated using U937-luc cells. CAR19-bi-BP T cells had very potent cytotoxic activity against U937 cells down to a 1:1 E:T ratio. The CAR-CLEC12A-2H3 T cells had similar potency in this assay. These data show that CAR19 T cells secreting CLEC12A-targeting BPs can kill an AML cell line, U937 with activity as potent as anti-CLEC12A CAR T cells (**Fig. 2E**).

To directly compare the CLEC12A-bridging CAR19 T cells to the CAR-CLEC12A T cells, transduced T-cell preparations were normalized to be 48% CAR-positive, with the exception of the CAR19-2H3-BP T cells, which were 44% CAR-positive. BP secretion was measured in these matched cell culture supernatants after a 4-day assay using anti-CD3/anti-CD28 activation of 600,000 cells/well. Average BP secretion ranged from 7.6 to 17 ng/mL (Supplementary Table S4). Next we used the U937 cytotoxicity assay to assess the activity of the CLEC12A-bridging CAR19 T cells from different donors (E:T at 3:1). CAR19-bi-BP T cells effectively killed the target cells (82%–100%) regardless of the donor although the amount of IFNγ secreted was highly variable (17.9–44.5 pg/mL, Supplementary Table S4). CAR19-scFv-BP T cells

were significantly less effective than the CAR19-bi-BP T cells ($P < 0.01$), inducing 44.2% cytotoxicity at the 3:1 E:T ratio ($n = 2$, 44% CAR-positive cells; Supplementary Table S4). The CAR-CLEC12A T cells routinely had cytotoxic activity >80% when tested at the 3:1 E:T ratio (Supplementary Table S4). This assay showed that CAR19-bi-BP T cells from different donors were highly potent.

Restimulation assay

Potent cell therapeutics engage in multiple rounds of tumor cell cytotoxicity, that is, serial killing. Here we used CLEC12A-bridging CAR19 T cells to model serial restimulation. U937 cells and Raji cells were used as target cells. There were treated with mitomycin-C to prevent cell division, as described previously (10). CAR19-bi-BP T cells were stimulated every 4 days then rested, through four rounds. Cell counts were obtained after each round, and aliquots of the recovered cells were used in cytotoxicity assays.

CAR19-bi-BP T cells restimulated with Raji cells expanded 15-fold in total cell number while the cells restimulated with U937 cells expanded 4-fold in total cell number (Supplementary Fig. S3A). Despite the difference in expansion, the recovered cells had very similar cytotoxic activities. CAR19-bi-BP T cells robustly killed U937 target cells after all four rounds of restimulation regardless of the cell type used to restimulate the CAR T cells (Raji or U937; Supplementary Fig. S3B). Similarly, CAR19-bi-BP T cells robustly killed CD19-positive JeKo-1 target cells after four rounds of restimulation regardless of the cell type used to restimulate the CAR T cells (Raji or U937; Supplementary Fig. S3C). T-cell populations were analyzed for effector status and PD-1 expression prior to, and after four rounds of restimulation. No significant differences were identified (Supplementary Table S5). These results show that CAR19-bi-BP T cells are able to serially engage target cells.

Activity of CAR19 T cells secreting CLEC12A-bringing proteins *in vivo*

Next, we evaluated the activity of CLEC12A-bridging CAR19 T cells *in vivo*. NSG mice were injected intravenously with 1×10^6 CD19-positive Nalm6-luc cells. Nalm6 cells rapidly disseminated, seeding the bone marrow and then developing into a systemic, lethal leukemia. Mice were treated 3 days after the Nalm6 injection with 2, 5, or 10×10^6 CAR19-bi-BP T cells/mouse. Control cohorts were injected with UTD T cells from the same donor (#38, 64% CAR-positive) or were not given T cells (NA). At day 21, the control animals were euthanized because of tumor burden (**Fig. 3A**). The two highest doses of CAR19-bi-BP T cells eliminated the leukemia and prevented lethality, and very little luminescence was detected (**Fig. 3A** and **B**). This indicated that the CLEC12A-bridging CAR19 T cells recognized CD19 directly, and that the secretion of the BP did not impair this activity *in vivo*. Previously we reported on additional cohorts from this study; images obtained on day 21 are shown for comparison and illustrate a second example using Her2-bridging CAR19 T cells (**Fig. 3C**; ref. 10).

Two models of aggressive systemic AML were tested. The U937 myeloid leukemia model is difficult to control and quickly lethal in NSG mice. In this study, the CLEC12A-bridging CAR19 T cells and the CAR-CLEC12A-scFv T cells were tested at different doses given 3 days after leukemia inoculation. The CAR T cells were made using donor #38, as used in the Nalm6 model. Doses of CAR T cells ranged from 2–10×10^6/animal. In this experimental setting all doses appeared equivalent by total luminescence measured through day 20, at which time the control cohorts (UTD and NA, $n = 10$ in total) had to be euthanized (**Fig. 3D**). This study demonstrated that the CAR19-bi-BP T cells had activity very similar to CAR-CLEC12A-scFv T cells.
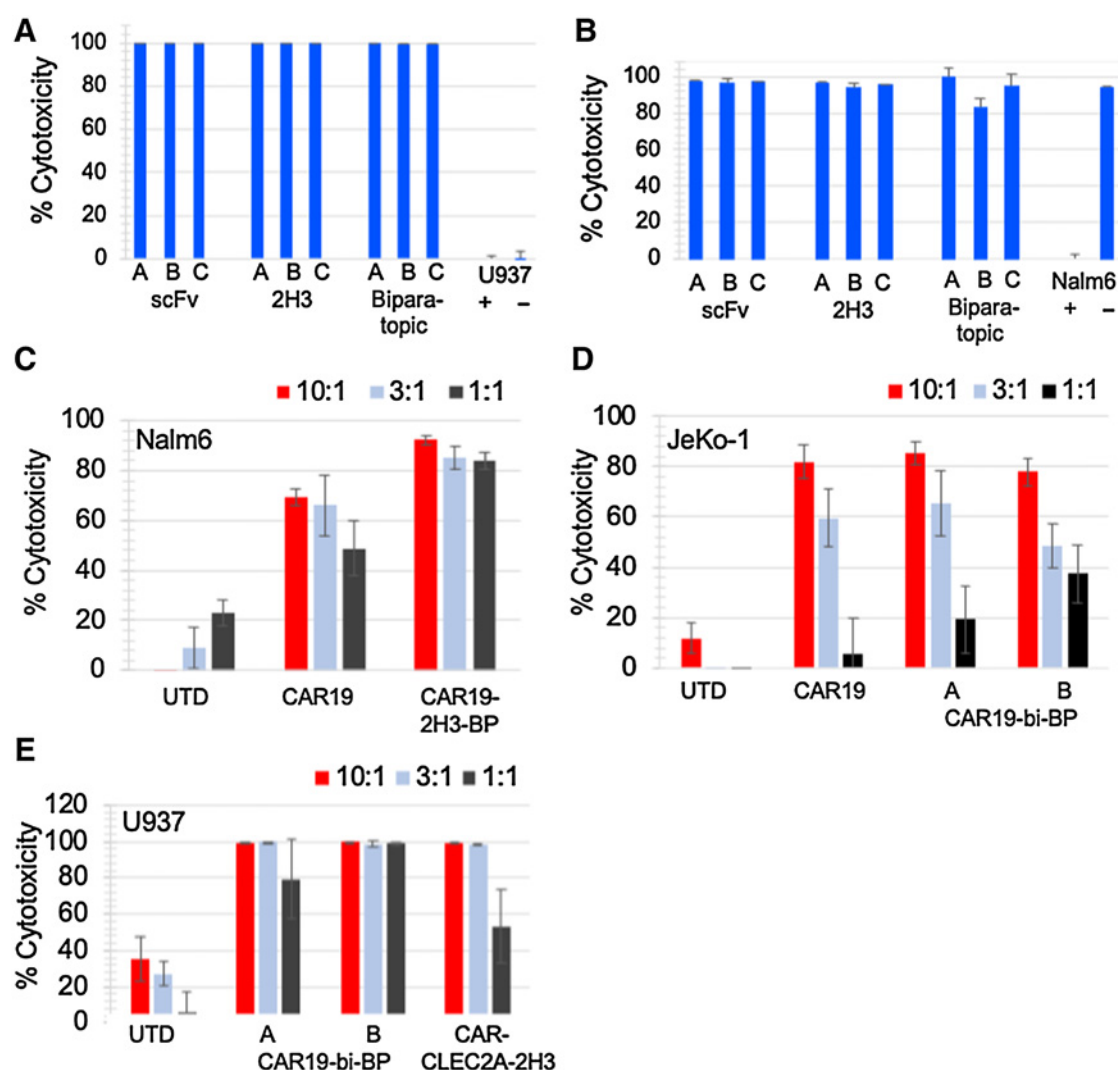
Figure 2.
Activity of CAR19 T cells in the presence of BPs. **A** and **B,** High BP concentration does not interfere with CAR19 T-cell–mediated killing. The three conditions indicated are BP prebound to CAR T cells (**A**), BP prebound to tumor cells (**B**), and BP, CAR T cells, and tumor cells added together simultaneously (**C**). The target tumor cells were U937-luc cells (**A**) or Nalm6-luc cells (**B**). **C–E,** The cytotoxic activity of CAR19 T cells and CAR19 T-cell–secreting BPs is shown. **C,** CAR19 T cells (47% CAR-positive) and anti-CD19 CAR-bi-BP T cells (50% CAR-positive) were mixed with Nalm6-luc cells at the indicated E:T ratios, and cytotoxicity was measured. The T cells were from donor 54. **D** and **E,** CAR19 T cells, CAR-CLEC12A-2H3 T cells, and CAR19-bi-BP T cells (each 50% CAR-positive, donor 18) were mixed with JeKo-1-luc cells (**D**) or U937-luc cells (**E**) at the indicated E:T ratios, and cytotoxicity was measured. In **D** and **E**, the CAR19-bi-BP designations refer to His-tagged, A, and untagged, B, forms.

An additional study was performed using the same conditions for U937 leukemia inoculation and addition of CAR19-bi-BP T cells from different donors (#38, as above, and donor #45, 55% CAR-positive). Sixty percent of the control animals had to be euthanized by day 20 and the rest by day 23 whereas the CAR19-bi-BP T-cell cohort had greatly reduced tumor burden and all but one animal survived through day 28 (**Fig. 3E** and **F**).

We assessed treatment of a different AML cell line, PL21, using the CLEC12A-bridging CAR19 T cells and CAR-CLEC12A T cells, both derived from donor #45, as used in the previous experiment. Control cohorts were treated with donor-matched UTD or CAR19 T cells or were untreated. NSG mice were inoculated with PL21 cells intravenously and the leukemia was allowed to disseminate and establish disease for 7 days prior to inoculation with CAR T cells. Animals were

imaged weekly to monitor disease progression (**Fig. 4**). By day 13, all control cohort mice ($n = 18$ total) showed clear luminescent signal in the femurs and lungs, whereas the animals in the CLEC12A-bridging anti-CD19 CAR and CAR-CLEC12A–treated cohorts only had a faint luminescent signal at the intravenous injection site in the tail (**Fig. 4C**). At day 28, all control mice had a systemic luminescent signal (**Fig. 4A** and **B**), and by the following week the control animals were humanely euthanized as they approached a signal of approximately 1×10^9 lumins/animal, at which time they showed signs of declining health (**Fig. 4C**).

A CLEC12A and CD33 bispecific BP

AML is a highly heterogeneous disease with variable antigen expression across and within subtypes (18, 23, 24). This led us to
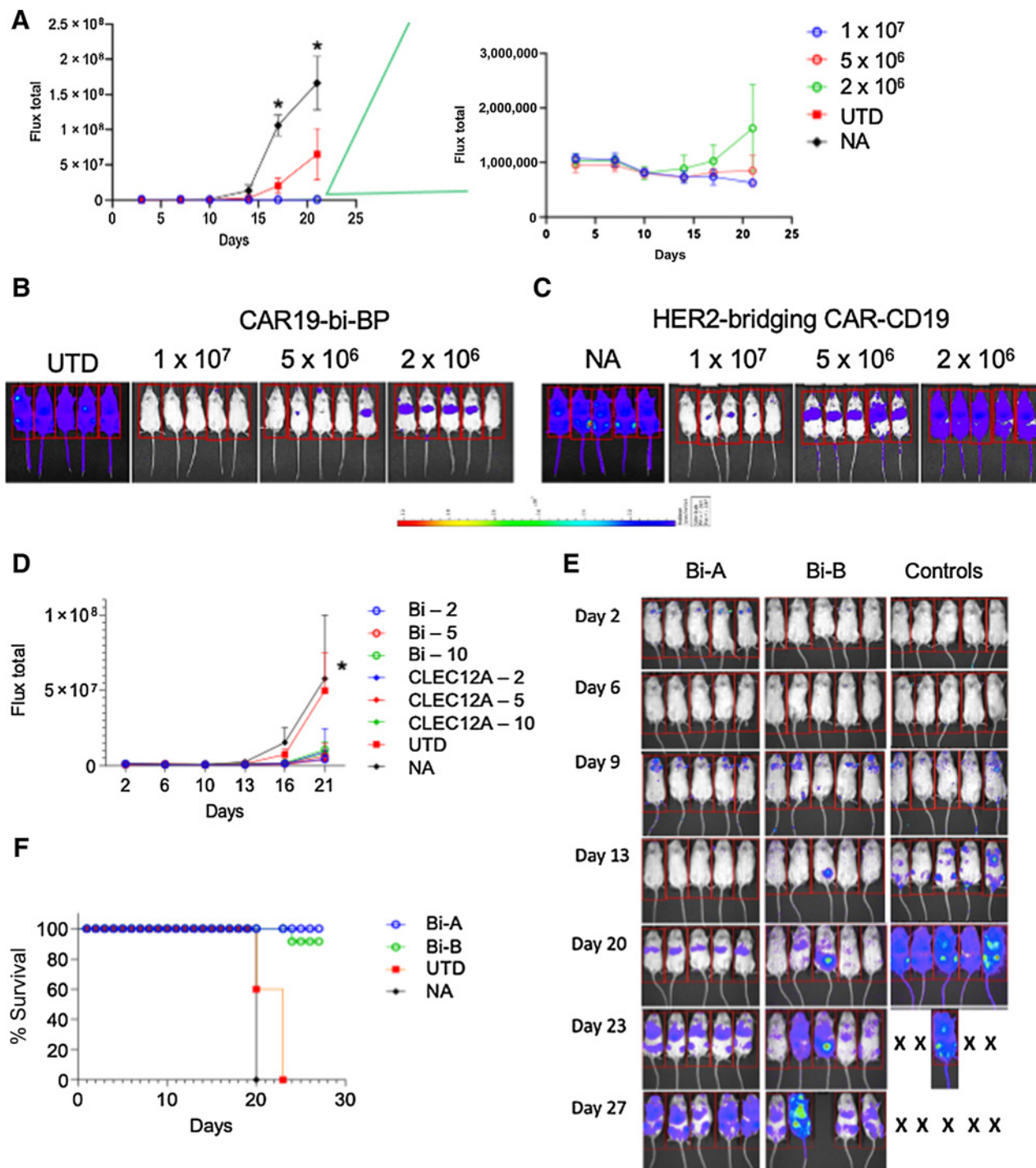
Figure 3.
In vivo models of CAR T cell activity. NSG mice were injected IV with Nalm6 cells and 3 days later given 2, 5, or 10 × 10^{6} CAR19-bi-BP T cells or UTD cells or no cells (NA). **A,** All three doses of CAR19-bi-BP T cells reduced the CD19-positive leukemia. The inset graph to the right shows the CAR19-bi-BP dose cohorts in greater detail; the two highest doses eradicated the CD19-positive tumor cells. **B** and **C,** Images showing protection from leukemia achieved with the CLEC12A-bridging anti-CD19 T cells compared with HER2-bridging CAR19 T cells. **D,** Three doses of CAR19-bi-BP T cells (2, 5, or 10 × 10^{6}) were compared with the same doses of CAR-CLEC12A-2H3 T cells in the U937 model. **E** and **F,** CAR19-bi-BP CAR T cells given at the 10 × 10^{6} dose improved survival in the U937 model (A: tagged, B: untagged). *, $P < 0.01$ for treatment cohorts compared with NA or with UTD; **, $P < 0.05$ for the lowest dose compared with the two higher doses. X = euthanized.

Figure 4.
CAR T-cell activity in the PL21 *in vivo* model. **A,** Graph of luminescent values in each cohort through day 40. **B,** Survival curve for each cohort through day 50. **C,** Individual animal images through day 44. X = euthanized. *, $P < 0.01$ and **, $P < 0.05$ for treatment cohorts compared with NA cohort.

create a BP with anti-CLEC12A and anti-CD33 binding capability. Sequences from the anti-CLEC12A 2H3 VH and an anti-CD33 scFv were combined with a stabilized CD19 to generate a dual-antigen BP (**Table 1**). Binding of the dual-antigen BP to both antigens, CLEC12A and CD33, remained intact and with approximately the same EC_{50} values as single antigen BPs (Supplementary Fig. S4A; **Table 1**). The AML cell lines PL21, AML2, and AML5 express variable levels of the antigens CD33 and Clec12A (Supplementary Fig. S4A). The dual-antigen BP bound to these cell lines with high affinity and mediated potent cytotoxicity by CAR19 T cells (Supplementary Fig. S4B and S4C). U937 cells express both CD33 and CLEC12A, but not CD19 (Supplementary Fig. S4A). The single and dual-antigen BPs bound to U937 cells with high affinity and mediated potent cytotoxic activity in the presence of CAR19 T cells (Supplementary Fig. S4D and S4E; Supplementary Table S6).

The Molm14 AML cell line expresses high levels of CD33 but little CLEC12A (Supplementary Fig. S4A). The binding of the single and dual-antigen BPs reflected this antigen expression (Supplementary Fig. S4F). A cytotoxicity assay using Molm14 cells showed that the dual-antigen BP mediated cytotoxic activity in the presence of CAR19 T cells similar to that of the anti-CD33 BP (Supplementary Fig. S4G). We compared the binding of the biparatopic and dual-antigen BPs on Molm14 cells. Biparatopic BP binding was very low; the dual-antigen BP bound to saturation (Supplementary Fig. S4H). In cytotoxicity assays, the dual-antigen BP demonstrated potent killing while the biparatopic BP failed to kill all target cells (Supplementary Fig. S4I).

The cell lines PL21, AML2, AML5, U937, and Molm14 do not express CD19 (Supplementary Fig. S5).

The CLEC12A-CD33 dual-antigen BP did not exhibit enhanced killing of cells expressing both antigens; however, both antigens clearly bound to the BP and mediated anti-CD19 CAR cytotoxicity. Further optimization of this BP design may support synergistic binding. Such dual-antigen BPs will be useful to target AML cells that do not express one of the antigens or downregulate one during the course of disease response to therapy.

Discussion

Here we have shown (i) a biparatopic CD19-anti-CLEC12A BP containing two distinct binders improves binding affinity, (ii) CD19-anti-CLEC12A BPs trigger CAR19 T cells to kill CLEC12A-positive AML cells *in vitro*, and (iii) CLEC12A-bridging CAR19 T cells kill AML cells *in vitro* and *in vivo* as potently as conventional CAR-CLEC12A T cells. These results confirm the robustness of this technology.

AML is a heterogeneous collection of hematopoietic stem cell–derived malignancies that can differ by LSC stage, by critical driver mutations, by oncogenic translocations, by epigenetic status and by expression of cell surface antigens. Despite this variability, most patients are given standard chemotherapy regimens, and then newer therapeutics in the refractory setting. The majority of patients eventually relapse and the 5-year survival rate is very low.

It is against this treatment landscape that CAR T-cell therapies for r/r AML are being developed; such efforts have been extensively reviewed (7, 13). CAR T antigen selection is a critical tolerability issue as AML antigens can also be expressed on mature myeloid lineage cells and on hematopoietic stem cells in the bone marrow (7). For example, CAR T cells targeting CD123 eliminate not just AML cells but also mature normal myeloid subsets and disrupt myelopoiesis, causing profound myelosuppression. CD123 is also expressed on other normal cell types. This highlights the importance of antigen selection.

Unfortunately, the heterogeneous pattern of AML antigen expression suggests that multi-antigen targeting will be critical for the successful development of durable and curative cellular therapies. Indeed, the issue of tumor antigen loss in response to cell therapy is observed across hematologic and solid tumor indications (3, 25, 26) and limits the utility of single antigen targeting CAR T cells.

The CLEC12A antigen has a particularly promising expression profile in AML with uniform and stable expression on blasts and LSCs across many subtypes (14, 15, 18, 27–29). Expression is not altered by standard therapy, for example, chemotherapy, and is stable from diagnosis through treatment through relapse. Importantly,

CLEC12A is not expressed on normal hematopoietic stem cells (14, 28, 29). Therefore, targeting the CLEC12A antigen will target AML blasts and LSCs while sparing normal hematopoiesis. Several groups have advanced CLEC12A-targeting CAR T cells into clinical trials (30, 31).

Our results demonstrate that targeting CLEC12A eliminates AML cells *in vitro* and significantly reduces tumor burden *in vivo*. In particular, the anti-CLEC12A biparatopic BP mediated anti-CD19 CAR cytotoxicity at low pmol/L concentrations, which is in the range of low to sub ng/mL levels in solution. The BP therefore acts like a CAR-T cell engager, with potency similar to that of blinatumumab acting as a T cell engager, as one example. Furthermore, we have engineered the CAR19 T cell itself to secrete the BP constitutively, at a level more than two logs above the effective IC_{50} concentration. This expression level, coupled with the low pmol/L affinity of the biparatopic BP for CLEC12A-expressing cells, ensures effective bridging and cytotoxicity. As a result, CAR19 T cells secreting the BP are as potent as anti-CLEC12A CAR T cells (**Fig. 4A**) while retaining all the advantages of CAR19 T cells themselves, including the inherent fitness and persistence characteristics that come from engaging CD19 on B cells (see below).

Notably, among the AML subtypes are several that express CD19 itself. Mixed phenotype leukemias (MPAL) are hematopoietic lineage malignancies that express both myeloid and lymphoid lineage markers. B-lineage MPAL can arise *de novo* (as a primary malignancy) or as a consequence of treatment of ALL (a lineage switch; ref. 32). This and other previously unclassified AML subtypes are also CLEC12A positive (18). Another AML subgroup that expresses both CLEC12A and CD19 is the t(8;21)(q22;q22) chromosomal abnormality (33); this subtype represents 10%–20% of all AML in adults and children.

Several efforts have been made to demonstrate the utility of targeting CD19 in these subgroup, including preclinical work and clinical case work with a CD19-targeting CAR (34, 35), and clinical case work using the CD3 × CD19 bispecific antibody blinatumomab (36). A very recent finding that CD19 is even more widely expressed in AML highlights the potential broad applicability of this dual-antigen targeting strategy (37). In CLEC12A-positive/CD19-positive AML, the CLEC12A-bridging CAR19 T cells will target both antigens through the anti-CD19 CAR domain.

The heterogeneity of antigen expression in AML, even within an individual patient, is a notable challenge for any therapeutic targeting a single antigen (37). In addition to CLEC12A, another important AML antigen is CD33, which is expressed broadly across AML subtypes. It has been reported that the percentage of adult patient samples that are dual positive for CLEC12A and CD33 is at least 70%, and the percentage positive for either CLEC12A or CD33 approached 95% (14, 28, 29). A recent analysis documented the high level of expression of CLEC12A and CD33 on AML patient cells as compared with normal cells and noted that these two antigens together are expressed by nearly all pediatric AML (38). Therefore, targeting both CLEC12A and CD33 should be broadly effective in most patients with AML. As a proof of concept, we engineered a dual-antigen BP containing two domains, one recognizing CLEC12A and a second recognizing CD33. This BP successfully mediated cytotoxicity against cells expressing either antigen (Supplementary Fig. S3). Because we have used an anti-CLEC12A VH and an anti-CD33 scFv, the overall size of the BP is small. The sequence of such dual antigen binders is short enough to be incorporated into lentiviral vectors and secreted by CAR19 T cells. Of note, CD33 is expressed on normal myeloid lineage cells and myeloid hematopoietic stem cells although at lower levels than on AML cells (38). The hypothesis that CAR T cells targeting

CD33 will induce myelosuppression as a side effect is currently being tested in early clinical trials; results are not yet available. Long-term data following patients treated with gentuzumab ozogamicin, and anti-CD33 antibody–drug conjugate, showed that while most patients experienced neutropenia and thrombocytopenia the incidence of grade 3/4 infections and bleeding events was low (39). Local secretion and the short half-life of CAR T engagers should further enhance tolerability. One group has reported development of a CD33 × CLEC12A CAR T cell (40). Other targets currently being evaluated in proof-of-concept BPs include B7H6 and IL1-RAP (41, 42).

CLEC12A-bridging CAR19 T cells are able to bind to CD19 on normal B cells. This is a critical feature because CAR T cells that are stimulated by B cells appear functionally superior to CAR T cells that are stimulated by tumor cells, whether solid tumors (10) or AML cells. In particular, CLEC12A-bridging CAR19 T cells expanded 15-fold through four rounds of restimulation using Raji cells but only expanded 4-fold when restimulated using U937 cells. While the restimulated CAR T cells retained cytotoxicity, there was a statistically significant drop in the extent of target cell killing after four rounds of restimulation with U937 versus Raji (**Fig. 3**; $P < 0.05$). A similar finding was reported in the context of anti-ROR1 CAR T cells that have been given to solid tumor patients and shown short persistence, in contrast to the behavior of those same CAR T cells in patients with chronic lymphocytic leukemia (43). Our current efforts are directed to understanding the mechanistic basis for these differences.

Several studies have suggested that normal B cells are critical for successful CAR19 T-cell therapy for B-cell malignancies. In syngeneic B-cell tumor models, tumor growth control by CAR19 T cells required the presence of normal B cells (44, 45). The clinical relevance of normal B cells to successful CAR19 T-cell therapy was shown in an analysis of B-cell leukemia treatment. It was demonstrated that a bone marrow composition of >15% of CD19-expressing cells (leukemia cells and normal B cells) prior to lymphodepletion was a primary factor driving CAR T expansion and persistence (46, 47). These data are consistent with a key role for normal CD19-positive B cells in supporting CAR19 T cell activity. Normal B cells provide immunologically relevant stimulatory signals to T cells, including costimulatory interactions, adhesion molecule interactions, and chemokine and cytokine signaling; the role of adhesion molecules supporting effector T-cell differentiation is an area of intense investigation (48–51). Also, B cells are a persistent and self-renewing antigen source. Thus, normal B cells can provide a non-tumor cell-dependent antigen depot that maintains the antitumor cell therapy until the target malignancy is completely eliminated and no residual disease remains. In AML, the goal is always to eliminate the last remaining blast and last remaining LSC that may be resident in the bone marrow. To achieve deep residual disease-negative status, it is ideal for the cell therapeutic to last longer than the malignancy. Indeed, as the periphery is depleted of AML cells and normal B cells, we would expect the CAR19 T cells to be found mainly in the bone marrow, which is where CD19-positive early B cells are released. In AML, this is exactly where we want the cell therapy to be located, because this is where the myeloid leukemia stem cells that are the source of AML relapse reside. Data from clinical studies using therapeutics in lymphomas and multiple myeloma are consistent with the hypothesis that CAR T cells can overcome local immunosuppression and survive harsh tumor microenvironments (1, 2). The BPs we develop undergo typical protein analytic evaluation during the lead development process, such analyses ensure serum stability, high Tm, stability in high and low pH, oxidation resistance, and other critical protein engineering characteristics (52). In addition, the CD19 ECD was screened to have excellent stability and protease resistance (9).

In summary, we have shown that multi-domain BPs can be used to redirect CAR19 T cells to target CLEC12A expressed by AML cells. The use of CD19-based BPs allows us to leverage the inherent fitness and persistence properties of CAR19 T cells. The flexibility of our modular platform is illustrated by the creation of a biparatopic anti-CLEC12A BP and of a dual antigen-targeting BP that can bind to both CLEC12A and CD33. The results presented here are a significant step toward our ultimate goal of combining small multi-antigen targeting CD19-based BPs with CAR19 T cells in multiple formats, including secretion from the CAR T cells themselves, secretion from tumor-specific viruses, and as injectable biologics. By this means, we anticipate significant efficacy can be achieved by thwarting antigen escape and resistance while leveraging the singular CAR19 T cell, whether autologous or allogeneic, and without the need for extensive genetic manipulation.

Authors' Disclosures

Authors' Contributions

P.D. Rennert: Conceptualization, supervision, funding acquisition, writing–original draft, writing–review and editing. **F.J. Dufort:** Investigation, methodology. **L. Su:** Investigation, methodology. **T. Sanford:** Investigation, methodology. **A. Birt:** Investigation, methodology. **L. Wu:** Investigation, methodology. **R.R. Lobb:** Conceptualization, funding acquisition. **C. Ambrose:** Conceptualization, formal analysis, supervision, investigation, methodology, writing–review and editing.

Acknowledgments

References

1. Frigault MJ, Maus MV. State of the art in CAR T cell therapy for CD19+ B cell malignancies. J Clin Invest 2020;130:1586–94.
2. Gagelmann N, Ayuk F, Atanackovic D, Kroger N. B cell maturation antigen-specific chimeric antigen receptor T cells for relapsed or refractory multiple myeloma: a meta-analysis. Eur J Haematol 2020;104:318–27.
3. Majzner RG, Mackall CL. Tumor antigen escape from CAR T-cell therapy. Cancer Discov 2018;8:1219–26.
4. D'Agostino M, Raje N. Anti-BCMA CAR T-cell therapy in multiple myeloma: can we do better? Leukemia 2020;34:21–34.
5. Roddie C, O'Reilly M, Dias Alves Pinto J, Vispute K, Lowdell M. Manufacturing chimeric antigen receptor T cells: issues and challenges. Cytotherapy 2019;21:327–40.
6. Neelapu SS. Managing the toxicities of CAR T-cell therapy. Hematol Oncol 2019;37:48–52.
7. Tasian SK. Acute myeloid leukemia chimeric antigen receptor T-cell immunotherapy: how far up the road have we traveled? Ther Adv Hematol 2018;9:135–48.
8. Watanabe K, Kuramitsu S, Posey AD Jr, June CH. Expanding the therapeutic window for CAR T cell therapy in solid tumors: the knowns and unknowns of CAR T cell biology. Front Immunol 2018;9:2486.
9. Klesmith JR, Su L, Wu L, Schrack IA, Dufort FJ, Birt A, et al. Retargeting CD19 chimeric antigen receptor T cells via engineered CD19-fusion proteins. Mol Pharm 2019;16:3544–58.
10. Ambrose C, Su L, Wu L, Dufort FJ, Sanford T, Birt A, et al. Anti-CD19 CAR T cells potently redirected to kill solid tumor cells. PLoS One 2021;16:e0247701.
11. Short NJ, Konopleva M, Kadia TM, Borthakur G, Ravandi F, DiNardo CD, et al. Advances in the treatment of acute myeloid leukemia: new drugs and new challenges. Cancer Discov 2020;10:506–25.
12. Anthias C, Dignan FL, Morilla R, Morilla A, Ethell ME, Potter MN, et al. Pre-transplant MRD predicts outcome following reduced-intensity and myeloablative allogeneic hemopoietic SCT in AML. Bone Marrow Transplant 2014;49:679–83.
13. Hofmann S, Schubert ML, Wang L, He B, Neuber B, Dreger P, et al. Chimeric antigen receptor (CAR) T cell therapy in acute myeloid leukemia (AML). J Clin Med 2019;8:200.
14. Perna F, Berman SH, Soni RK, Mansilla-Soto J, Eyquem J, Hamieh M, et al. Integrating proteomics and transcriptomics for systematic combinatorial chimeric antigen receptor therapy of AML. Cancer Cell 2017;32:506–19.
15. Haubner S, Perna F, Kohnke T, Schmidt C, Berman S, Augsberger C, et al. Coexpression profile of leukemic stem cell markers for combinatorial targeted therapy in AML. Leukemia 2019;33:64–74.
16. Bill M, van Kooten Niekerk PB, Woll PS, Laine Herborg L, Stidsholt Roug A, Hokland P, et al. Mapping the CLEC12A expression on myeloid progenitors in normal bone marrow; implications for understanding CLEC12A-related cancer stem cell biology. J Cell Mol Med 2018;22:2311–8.
17. Walter RB, Appelbaum FR, Estey EH, Bernstein ID. Acute myeloid leukemia stem cells and CD33-targeted immunotherapy. Blood 2012;119:6198–208.
18. Bakker AB, van den Oudenrijn S, Bakker AQ, Feller N, van Meijer M, Bia JA, et al. C-type lectin-like molecule-1: a novel myeloid cell surface marker associated with acute myeloid leukemia. Cancer Res 2004;64:8443–50.
19. Ciccarese S, Burger PA, Ciani E, Castelli V, Linguiti G, Plasil M, et al. The camel adaptive immune receptors repertoire as a singular example of structural and functional genomics. Front Genet 2019;10:997.
20. Goebeler ME, Bargou RC. T cell-engaging therapies - BiTEs and beyond. Nat Rev Clin Oncol 2020;17:418–34.
21. Novosiadly R, Kalos M. High-content molecular profiling of T-cell therapy in oncology. Mol Ther Oncolytics 2016;3:16009.
22. Calderon H, Mamonkin M, Guedan S. Analysis of CAR-mediated tonic signaling. Methods Mol Biol 2020;2086:223–36.
23. Rose D, Haferlach T, Schnittger S, Perglerova K, Kern W, Haferlach C. Subtype-specific patterns of molecular mutations in acute myeloid leukemia. Leukemia 2017;31:11–7.
24. Launder TM, Bray RA, Stempora L, Chenggis ML, Farhi DC. Lymphoid-associated antigen expression by acute myeloid leukemia. Am J Clin Pathol 1996;106:185–91.
25. Timmers M, Roex G, Wang Y, Campillo-Davo D, Van Tendeloo VFI, Chu Y, et al. Chimeric antigen receptor-modified T cell therapy in multiple myeloma: beyond B cell maturation antigen. Front Immunol 2019;10:1613.
26. Akhavan D, Alizadeh D, Wang D, Weist MR, Shepphird JK, Brown CE. CAR T cells for brain tumors: lessons learned and road ahead. Immunol Rev 2019;290:60–84.
27. Ma H, Padmanabhan IS, Parmar S, Gong Y. Targeting CLL-1 for acute myeloid leukemia therapy. J Hematol Oncol 2019;12:41.
28. van Rhenen A, van Dongen GA, Kelder A, Rombouts EJ, Feller N, Moshaver B, et al. The novel AML stem cell associated antigen CLL-1 aids in discrimination between normal and leukemic stem cells. Blood 2007;110:2659–66.

29. Wang J, Chen S, Xiao W, Li W, Wang L, Yang S, et al. CAR-T cells targeting CLL-1 as an approach to treat acute myeloid leukemia. J Hematol Oncol 2018;11:7.

30. Cummins KD, Gill S. Chimeric antigen receptor T-cell therapy for acute myeloid leukemia: how close to reality? Haematologica 2019;104:1302–8.

31. Zhang H, Gan WT, Hao WG, Wang PF, Li ZY, Chang LJ. Successful anti-CLL1 CAR T-cell therapy in secondary acute myeloid leukemia. Front Oncol 2020; 10:685.

32. Charles NJ, Boyer DF. Mixed-phenotype acute leukemia: diagnostic criteria and pitfalls. Arch Pathol Lab Med 2017;141:1462–8.

33. Kita K, Nakase K, Miwa H, Masuya M, Nishii K, Morita N, et al. Phenotypical characteristics of acute myelocytic leukemia associated with the t(8;21)(q22;q22) chromosomal abnormality: frequent expression of immature B-cell antigen CD19 together with stem cell antigen CD34. Blood 1992;80:470–7.

34. Ma G, Wang Y, Ahmed T, Zaslav AL, Hogan L, Avila C, et al. Anti-CD19 chimeric antigen receptor targeting of CD19+acute myeloid leukemia. Leuk Res Rep 2018;9:42–4.

35. Danylesko I, Jacoby E, Yerushalmi R, Shem-Tov N, Besser MJ, Vernitsky H, et al. Remission of acute myeloid leukemia with t(8;21) following CD19 CAR T-cells. Leukemia 2020;34:1939–42.

36. Plesa A, Labussiere-Wallet H, Hayette S, Salles G, Thomas X, Sujobert P. Efficiency of blinatumomab in a t(8;21) acute myeloid leukemia expressing CD19. Haematologica 2019;104:e487–8.

37. Miles LA, Bowman RL, Merlinsky TR, Csete IS, Ooi AT, Durruthy-Durruthy R, et al. Single-cell mutation analysis of clonal evolution in myeloid malignancies. Nature 2020;587:477–82.

38. Willier S, Rothamel P, Hastreiter M, Wilhelm J, Stenger D, Blaeschke F, et al. CLEC12A and CD33 coexpression as a preferential target for pediatric AML combinatorial immunotherapy. Blood 2021;137:1037–49.

39. Leopold LH, Berger MS, Feingold J. Acute and long-term toxicities associated with gemtuzumab ozogamicin (Mylotarg) therapy of acute myeloid leukemia. Clin Lymphoma 2002;2:S29–34.

40. Liu F, Zhang H, Sun L, Li Y, Zhang S, He G, et al. First-in-human CLL1-CD33 compound CAR (CCAR) T cell therapy in relapsed and refractory acute myeloid leukemia. European Hematology Association 2020 Annual Meeting.

41. Przespolewski A, Szeles A, Wang ES. Advances in immunotherapy for acute myeloid leukemia. Future Oncol 2018;14:963–78.

42. Mitchell K, Barreyro L, Todorova TI, Taylor SJ, Antony-Debre I, Narayanagari SR, et al. IL1RAP potentiates multiple oncogenic signaling pathways in AML. J Exp Med 2018;215:1709–27.

43. Specht JM, Lee SM, Turtle C, Berger C, Balakrishnan A, Srivastava S, et al. A phase I study of adoptive immunotherapy for ROR1+ advanced triple negative breast cancer (TNBC) with defined subsets of autologous T cells expressing a ROR1-specific chimeric antigen receptor (ROR1-CAR) [abstract]. In: Proceedings of the 2018 San Antonio Breast Cancer Symposium; 2018 Dec 4-8; San Antonio, TX. Philadelphia (PA): AACR; Cancer Res 2019;79(4 Suppl): Abstract nr P2-09-13.

44. Yang Y, Kohler ME, Fry TJ. Effect of chronic endogenous antigen restimulation on CAR T cell persistence and memory formation. Blood 2017;130:166.

45. Cheadle EJ, Hawkins RE, Batha H, O'Neill AL, Dovedi SJ, Gilham DE. Natural expression of the CD19 antigen impacts the long-term engraftment but not antitumor activity of CD19-specific engineered T cells. J Immunol 2010;184: 1885–96.

46. Singh N, Frey NV, Grupp SA, Maude SL. CAR T cell therapy in acute lymphoblastic leukemia and potential for chronic lymphocytic leukemia. Curr Treat Options Oncol 2016;17:28.

47. Finney OC, Brakke HM, Rawlings-Rhea S, Hicks R, Doolittle D, Lopez M, et al. CD19 CAR T cell product and disease attributes predict leukemia remission durability. J Clin Invest 2019;129:2123–32.

48. Dustin ML. Role of adhesion molecules in activation signaling in T lymphocytes. J Clin Immunol 2001;21:258–63.

49. Commins SP, Borish L, Steinke JW. Immunologic messenger molecules: cyto-kines, interferons, and chemokines. J Allergy Clin Immunol 2010;125:S53–72.

50. Fooksman DR, Vardhana S, Vasiliver-Shamis G, Liese J, Blair DA, Waite J, et al. Functional anatomy of T cell activation and synapse formation. Annu Rev Immunol 2010;28:79–105.

51. Greenwald RJ, Freeman GJ, Sharpe AH. The B7 family revisited. Annu Rev Immunol 2005;23:515–48.

52. Ma H, O'Fagain C, O'Kennedy R. Antibody stability: a key to performance - analysis, influences and improvement. Biochimie 2020;177:213–25.